The 6th ASME-JSME Thermal Engineering Joint Conference
March 16-20, 2003

TED-AJ03-183

A MOLECULAR DYNAMICS SIMULATION OF WATER DROPLET IN CONTACT WITH A PLATINUM SURFACE

Tatsuto KIMURA
Department of Mechanical Engineering
The University of Tokyo
7-3-1 Hongo, Bunkyo-ku, Tokyo, 113-8656, Japan
E-mail: kimutatu@photon.t.u-tokyo.ac.jp

Shigeo MARUYAMA
Department of Mechanical Engineering
The University of Tokyo
7-3-1 Hongo, Bunkyo-ku, Tokyo, 113-8656, Japan
E-mail: maruyama@photon.t.u-tokyo.ac.jp

Keywords: Molecular Dynamics Method, Water, Platinum, Contact Angle

ABSTRACT

A water droplet in contact with a platinum surface was simulated by the molecular dynamics method. Water molecules were modeled with the well-known SPC/E model and the platinum surface was represented by three layers of harmonic molecules. The phantom molecules were used beneath the layers of platinum surface in order to mimic the constant temperature heat bath. As the potential function between water and platinum surface, two different models developed by Spohr & Heinzinger (1988) and Zhu & Philpott (1994) were employed. These potential models were derived from the extended Hükel calculations between a water molecule and a platinum cluster. As the initial condition, a water droplet with the density of liquid water at 350 K was placed on the center of the platinum surface. For the initial 100 ps, velocity scaling was used for the temperature control. After this initial rough control, only the phantom heat bath was used as the temperature control at 350K.

During the velocity-scaling temperature control in 100 ps, the liquid vapor interface was already in semi-spherical shape. Then, the gradual spreading of the water droplet was observed. In the spreading process of a liquid droplet on a platinum surface, the area of contact region between water and platinum expanded just in proportion to the one-third power of time at early stage and later to the one-fifth power of time. On the other hand, for Lennard-Jones fluid, it was reported that the spread of interfacial area was proportional to the logarithmic or square of time.

Even though the water droplet finally spread to a monolayer film on a fcc (111) surface with the S-H potential, a stable droplet structure on a monolayer film was realized with the Z-P potential as shown in Fig. A-1 and Fig. A-2. This is the first realization of stable droplet structure on the monolayer film with molecular dynamics level calculation. The mechanism of the 'drop on film' structure was explained by the very concentrated monolayer film of water. The dense monolayer repulses the other molecules, so that the effective potential of the surface is weakened. Hence, the layer concentration of the monolayer leads to the larger contact angle (less wettable).

Furthermore, comparing three different platinum surface structures, (111), (100) and (110), the contact angle varied drastically depending on the density of the monolayer and it was largest on the fcc (100) surface.

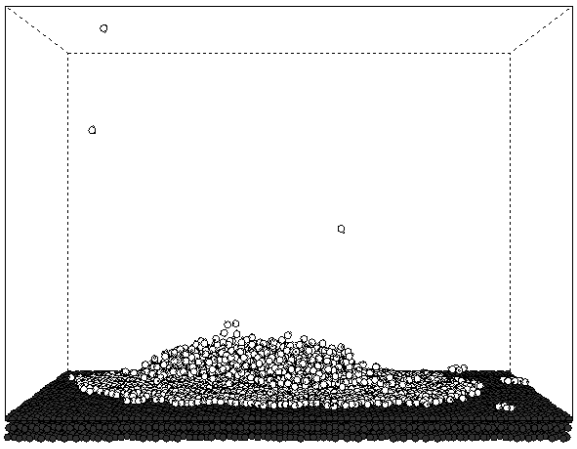

Figure A-1 Snapshot of water droplet on fcc(111) platinum surface (Z-P potential).

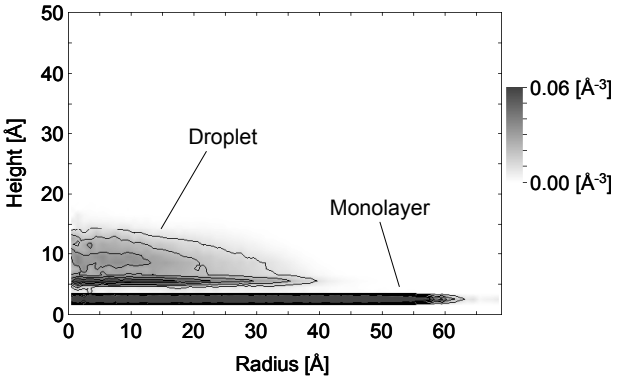

Figure A-2 Two-dimensional density profiles of water droplet on fcc (111) platinum surface (Z-P potential).

INTRODUCTION

Molecular level understanding of dynamics of liquid and solid contact is important for phase change heat transfer such as evaporation and condensation. We have simulated the equilibrium liquid droplet [1], vapor bubble nucleation [2], and liquid droplet nucleation [3] on the solid surface for the simple Lennard-Jones fluid system. By arbitrary changing the potential parameter between fluid and solid molecules, considerable information is obtained about the wetting of a surface. In practice, water is the most important molecule in engineering and in theoretical framework. Here, a molecular dynamics simulation of a water droplet on a platinum surface is performed. The spreading phenomena and final equilibrium structure of water on the surface were compared for two different water-platinum intermolecular potentials and different platinum surface lattice structures.

NOMENCLATURE

A = area of solid liquid interface
a = potential parameter of S-H potential
b = potential parameter of S-H potential
c = potential parameter of S-H potential
k = spring constant
m = mass
N = number of Molecules
q = electrical charge
r = distance
r_0 = nearest neighbor distance
t = time

Greek Symbols

α = potential parameter of Z-P potential
ε = potential parameter of Z-P potential
ϕ = potential function
ρ = length of the projection of the distance vector onto the surface plane
σ = potential parameter of Z-P potential

Subscripts

an = anisotropic
cond = conductance
H = hydrogen
H_2O = water molecule
isr = isotropic
O = oxygen
Pt = platinum
surf = surface

SIMULATION METHOD

The simulation system is shown in Fig. 1. Platinum surface was located at the bottom and mirror boundary condition at the top and periodic boundary conditions in 4 sides were employed. Water molecule was modeled with the well-known SPC/E model [4] and the platinum surface was represented by three layers of harmonic molecules. The phantom molecules [5,6] were used beneath the layers of platinum surface in order to mimic the constant temperature heat bath. Harmonic potential parameters for platinum atoms were set as k = 46.8 N/m and r_0 = 0.277 nm.

Two different potential functions between water and platinum surface were employed. Both potential models were derived from the extended Hückel calculations between a water molecule and a platinum cluster [7]. One is the model developed by Spohr and Heinzinger in 1988 [8]. The potential function is described as follows.

$$\phi_{H_2O-Pt} = \phi_{O-Pt}(r_{OPt}, \rho_{OPt}) + \phi_{HPt}(r_{H_1Pt}) + \phi_{H-Pt}(r_{H_2Pt}) \quad (1)$$

$$\phi_{O-Pt} = [a_1 \exp(-b_1 r) - a_2 \exp(-b_2 r)] f(\rho) + a_3 \exp(-b_3 r)[1 - f(\rho)] \quad (2)$$

$$\phi_{H-Pt} = a_4 \exp(-b_4 r) \quad (3)$$

$$f(\rho) = \exp(-c\rho^2) \quad (4)$$

where $a_1 = 1.8942\times10^{-16}$ J, $b_1 = 11.004$ nm^{-1},
$a_2 = 1.8863\times10^{-16}$ J, $b_2 = 10.966$ nm^{-1},
$a_3 = 10^{-13}$ J, $b_3 = 53.568$ nm^{-1},
$a_4 = 1.742\times10^{-19}$ J, $b_4 = 12.777$ nm^{-1},
$c = 11.004$ nm^{-1}

Here, r is inter-atomic distance, and ρ is the length of the projection of the distance vector onto the surface plane. This potential has the minimum value when a water molecule sits on top of a platinum atom with the dipole moment directing upward. Figure 2 shows configurations of small cluster of water on the surface. Because of the

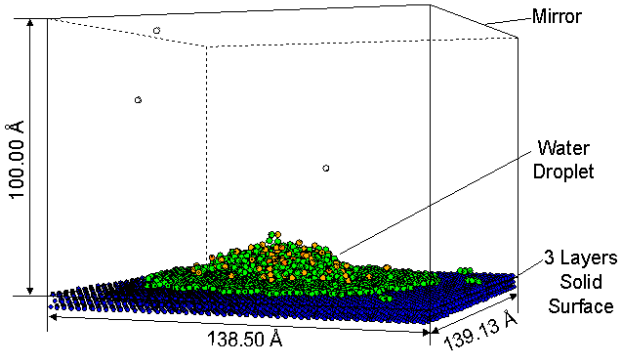

Figure 1 System configuration (2048 water droplet on fcc(111) platinum surface).

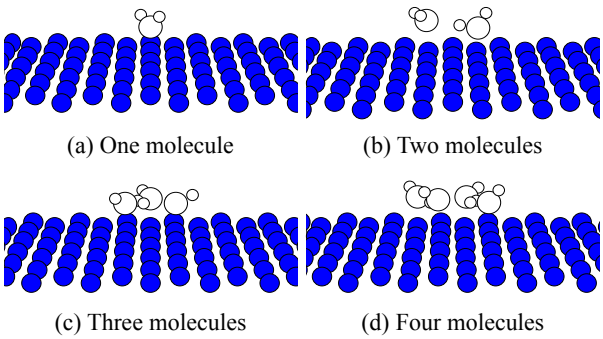

Figure 2 Small water clusters on fcc (111) platinum surface at 0K (S-H potential).

hydrogen bonding of water molecules, each water molecules has different orientation from the single water case.

The other potential model between water and platinum surface was developed by Zhu and Philpott (1994) [9]. The potential function consists of water molecule-conduction electron potential, anisotropic short-range potential and isotropic short-range r^{-10} potential as follows.

$$\phi_{\mathrm{H_2O-surf}} = \phi_{\mathrm{H2O-cond}} + \phi_{\mathrm{an}}(\mathrm{O};\mathbf{r}_{\mathrm{O}}) + \phi_{\mathrm{isr}}(\mathrm{O};\mathbf{r}_{\mathrm{O}}) + \sum_{H}\left[\phi_{\mathrm{an}}(\mathrm{H};\mathbf{r}_{\mathrm{H}}) + \phi_{\mathrm{isr}}(\mathrm{H};\mathbf{r}_{\mathrm{H}})\right] \quad (5)$$

$$\phi_{\mathrm{H2O-cond}} = \sum_{l,k}\frac{q_l q_k}{2r_{lk}} \quad (6)$$

$$\phi_{\mathrm{an}}(p;\mathbf{r}_p) = 4\varepsilon_{p-\mathrm{Pt}}\sum_j\left[\left(\frac{\sigma_{p-\mathrm{Pt}}^{\ 2}}{(\alpha\rho_{pj})^2 + z_{pj}^{\ 2}}\right)^6 - \left(\frac{\sigma_{p-\mathrm{Pt}}^{\ 2}}{(\rho_{pj}/\alpha)^2 + z_{pj}^{\ 2}}\right)^3\right] \quad (7)$$

$$\phi_{\mathrm{isr}}(p;\mathbf{r}_p) = -4\varepsilon_{p-\mathrm{Pt}}\sum_j\frac{c_{p-\mathrm{Pt}}\sigma_{p-\mathrm{Pt}}^{\ 10}}{r_{pj}^{\ 10}} \quad (8)$$

where $\alpha = 0.8$

$\sigma_{\mathrm{O\text{-}Pt}} = 0.270$ nm, $\varepsilon_{\mathrm{O\text{-}Pt}} = 6.44\times10^{-21}$ J, $c_{\mathrm{O\text{-}Pt}} = 1.28$

$\sigma_{\mathrm{H\text{-}Pt}} = 0.255$ nm, $\varepsilon_{\mathrm{H\text{-}Pt}} = 3.91\times10^{-21}$ J, $c_{\mathrm{H\text{-}Pt}} = 1.2$

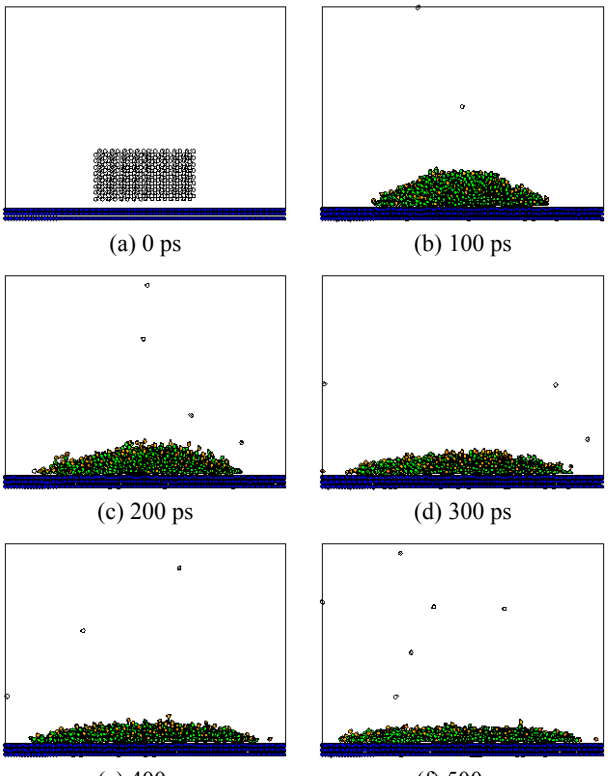

(a) 0 ps (b) 100 ps (c) 200 ps (d) 300 ps (e) 400 ps (f) 500 ps

Figure 3 Snapshots of water droplet on fcc(111) platinum surface (S-H potential, N=2048).

Equation (6) represents Coulomb potential between point charge of water molecule and its image charge located at symmetrical position below the image plane. This potential also has the minimum value when a water molecule sits on top of a platinum atom, but the binding energy is stronger than the S-H potential.

The well-known Ewald method is usually used for the long-range correction of the Coulomb potential [10]. However, we used the cut-off method [11] in order to increase the computational efficiency for this heterogeneous system. The large cut-off length of 25 Å between water and water molecules and 15 Å between water and platinum atoms were employed. The leapfrog method is used for the numerical integration of the equation of motion with the time step of 0.5 fs.

As the initial condition, an ice crystal with 864 or 2048 molecules with the density of bulk water at 350 K was placed on the center of the platinum surface. For the initial 100 ps, simple velocity scaling was used for the temperature control. After this initial rough control, only the phantom heat bath was employed as the temperature control at 350K.

RESULTS AND DISCUTIONS

Spreading of a water droplet on a platinum surface

Figure 3 shows snapshots of the water droplet with 2048 molecules on a fcc (111) platinum surface employing the Spohr-Heinzinger water-platinum potential. During the velocity scaling temperature control in 100 ps, the liquid vapor interface was already in spherical cap shape. Then, the gradual spreading of the water droplet was observed. Figure 4 shows the change in total dipole moment of the system. The increase of the total dipole moment is the good measure of the average orientation of water molecules. Since the contribution to the total dipole moment from a relatively free water molecule is large, the increase in the dipole moment shows the spreading. The smallest system with 864 water molecules reached the equilibrium at about 1000 ps with the almost constant

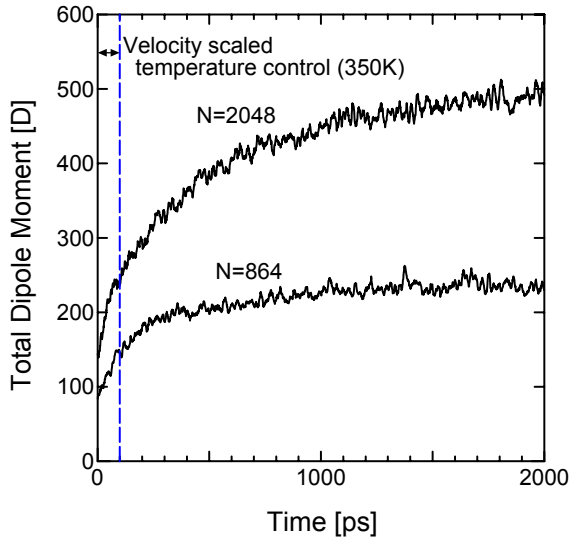

Figure 4 Variations of total dipole moment of the system (fcc (111), S-H potential).

total dipole moment. And for the larger 2048 system, the equilibrium was almost obtained at 2000 ps.

The spreading of the water droplet is measured in Fig. 5 as the area of water-platinum interface. Except for the initial 100 ps when the velocity-scaling temperature control was done, this change of the interface area was proportional to the one-third power of time at early stage and later to the one-fifth power of time. The broken curves and dotted curve are fit curves with $A \propto t^{1/3}$ and $A \propto t^{1/5}$, respectively. Inspired by the direct ellipsometric measurements of monolayer and terraced liquid film [12], spreading of liquid on completely wet surface has been studied extensively in this decade. Even though the experimentally assigned spreading rate was $A \propto t$, initial molecular dynamics simulations using the Lennard-Jones potential resulted in contradictory relations, $A \propto \log(t)$ [13] or $A \propto t^2$ [14], depending on the volatility or the surface conditions. More recent large-scale molecular dynamics simulations could predict the correct spreading rate; $A \propto t$ and extensive efforts of the modeling were being performed [15]. The much slower spreading rate of water on the platinum surface compared with the case of simple molecules is probably because of the large energy barrier of the contact line movement due to the commensuration of water layer to the platinum crystal.

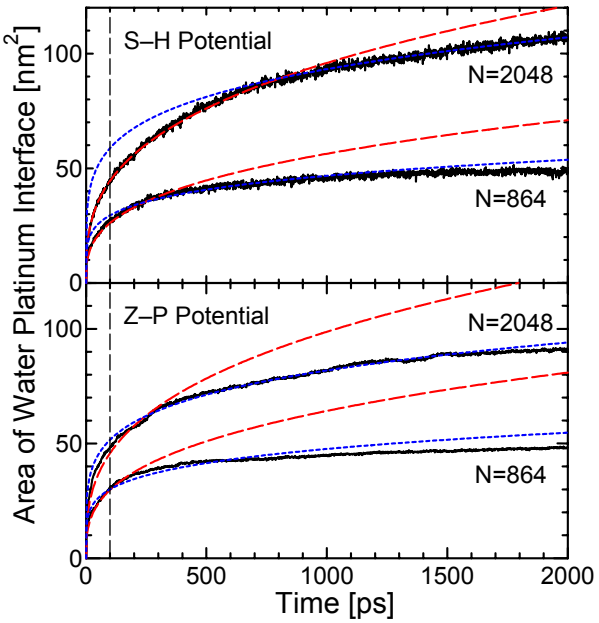

Figure 5 Expansion of water-platinum contact area on fcc (111) surface. The broken and dotted lines are fit curves with $A \propto t^{1/3}$ and $A \propto t^{1/5}$, respectively.

Structure of water droplet on platinum surface

Figure 6 shows the two-dimensional density distributions of the equilibrium water droplets. In the case of S-H potential, the droplet finally spread to almost monolayer and only a few molecules stayed on the film. On the other hand, in the case of the Z-P potential, a liquid droplet with a contact angle on the monolayer was observed. This is the first realization of stable droplet structure on the precursor film with molecular dynamics level calculation. Even though the existence of the precursor film is anticipated, the clear physical understanding of the three phase contact line has not been obtained. The simple relation obtained for the Lennard-Jones fluid was that the interface potential strength was proportional to the cosine of contact angle [1]. This could be readily imagined by the analogy to the Young's equation. However, the stronger interaction in the Z-P potential now resulted the less wetting structure compared with the S-H potential. The reason for this apparently controversial result can be explained as follows. The monolayer was very dense and there was space between the monolayer and the droplet. The dense monolayer repulses the other molecules, so that the effective potential between a platinum surface and the droplet on the monolayer is weakened. Hence, the layer concentration of the monolayer leads to the larger contact angle (less wettable).

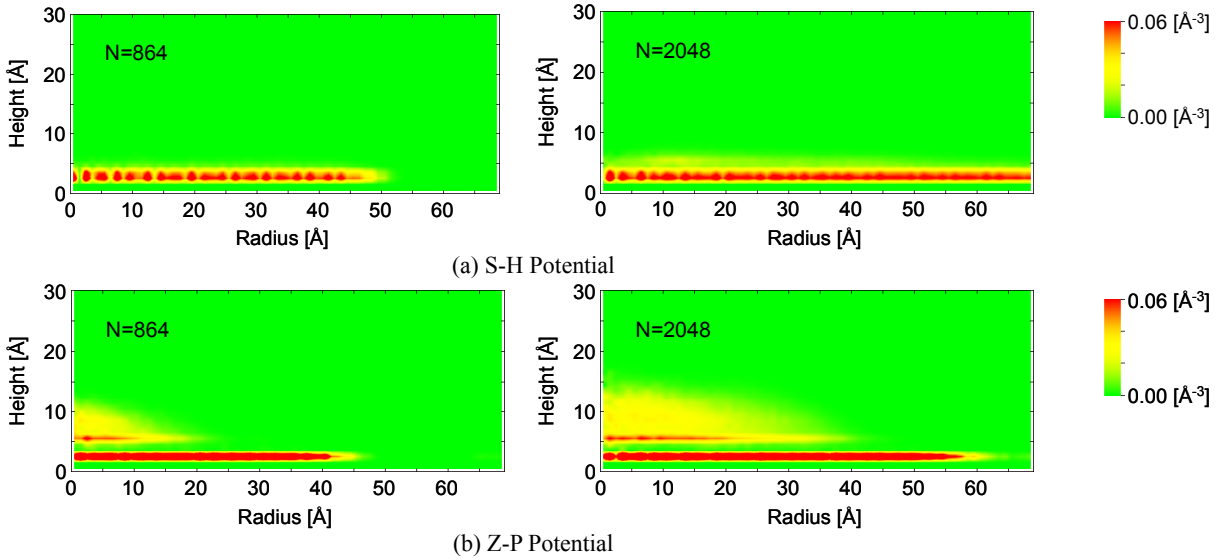

(a) S-H Potential

(b) Z-P Potential

Figure 6 Two-dimensional density profiles of water droplet on fcc (111) platinum surface.

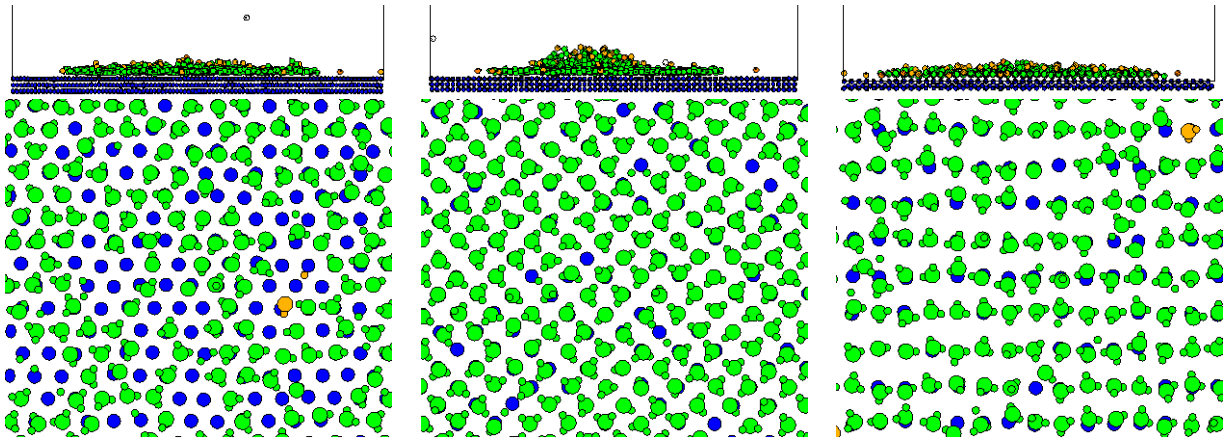

(a) fcc(111) (b) fcc(100) (c) fcc(110)

Figure 7 Snapshots of water droplet and its first layer (S-H potential).

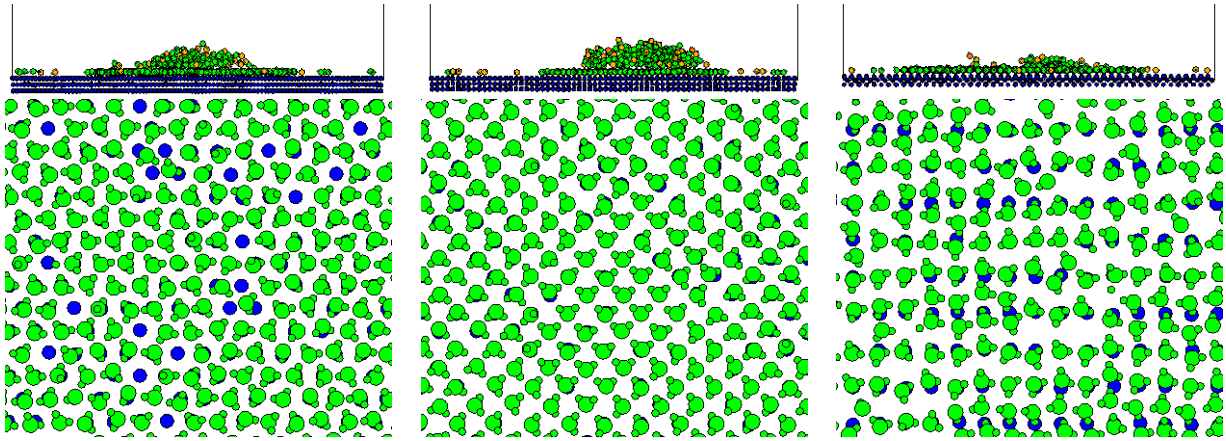

(a) fcc(111) (b) fcc(100) (c) fcc(110)

Figure 8 Snapshots of water droplet and its first layer (Z-P potential).

Figure 7 and Fig. 8 show snapshots of the water droplet and its first layer on different surface lattice structures employing the S-H potential and the Z-P potential, respectively. And Fig. 9 shows the density distribution of the first layer. The platinum surface atom density is largest for (111), medium for (100) and smallest for (110). For (100) and (110) surfaces, water molecules almost completely cover the platinum atoms. Hence, the water molecular density of monolayer is largest for the (100) surface, and the contact angle is the largest. In the case of the (110) surface, the platinum atom density is too low so that the contact angle is the smallest. These trends were valid for both the S-H (weaker) and Z-P (stronger) potentials. Hence, the explanation based on the monolayer density is completely valid.

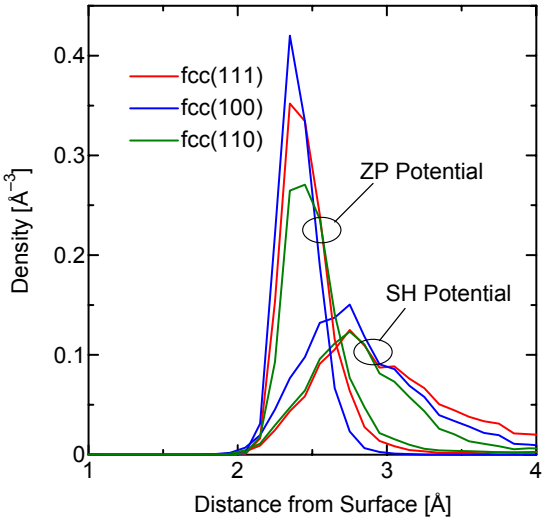

Figure 9 Density distribution of the first layer.

CONCLUSIONS

A molecular dynamics simulation of a water droplet on a platinum surface was performed. In the spreading process of water droplet, the area of contact region between water and platinum expanded just in proportion to the one-third power of time at early stage and later the one-fifth power of time. This speed is slower than the case of the Lennard-Jones liquid droplet. The final equilibrium shape of a water droplet was compared between two different water-platinum potentials and three different platinum surface lattice structures. With stronger water-platinum interaction, the contact angle became larger because of the repulsive effect of the dense monolayer. On the fcc (100) platinum surface, because of high coverage of water molecules on platinum atoms, the contact angle was largest.

ACKNOWLEDGEMENT

This work is supported by Grant-in-Aid for JSPS Fellows.

REFERENCES

[1] Maruyama, S., Kurashige, T., Matsumoto, S., Yamaguchi, Y., and Kimura, T., "Liquid Droplet in Contact with a Solid Surface", Microscale Thermophys. Eng., Vol. 2, No. 1 (1998), pp.49-62.

[2] Maruyama, S., and Kimura, T., "A Molecular Dynamics Simulation of a Bubble Nucleation on Solid Surface", Int. J. Heat & Technology, Vol. 18, Supp. 1 (2000), pp.69-74.

[3] Kimura, T., and Maruyama, S., "A Molecular Dynamics Simulation of Heterogeneous Nucleation of a Liquid Droplet on Solid Surface", Microscale Thermophys. Eng., Vol. 6, No. 1 (2002), pp.3-13.

[4] Berendsen, H. J. C., Grigera, J. R., and Straatsma, T. P., "The Missing Term in Effective Pair Potentials", J. Phys. Chem., Vol. 91, No. 24 (1987), pp.6269-6271.

[5] Tully, J. C., "Dynamics of Gas-surface Interactions: 3D Generalized Langevin Model Applied to fcc and bcc Surface", J. Chem. Phys., Vol. 73, No. 4 (1980), pp. 1975-1985.

[6] Blömer, J., and Beylich, A. E., "Molecular Dynamics Simulation of Energy Accommodation of Internal and Translational Degrees of Freedom at Gas-Surface Interfaces", Surf. Sci., Vol. 423 (1999), pp. 127-133.

[7] Holloway, S., and Bennemann, K. H., "Study of Water Adsorption on Metal Surfaces", Surf. Sci., Vol. 101 (1980), pp. 327-333.

[8] Spohr, E., and Heinzinger, K., "A Molecular Dynamics Study on the Water/Metal Interfacial Potential", Ber. Bunsenges. Phys. Chem., Vol. 92 (1988), pp. 1358-1363.

[9] Zhu, S.-B., and Philpott, M. R., "Interaction of Water with Metal Surfaces", J. Chem. Phys., Vol. 100, No. 9 (1994), pp. 6961-6968.

[10] Allen, M. P., and Tildesley, D. J., "Computer Simulation of Liquids", New York, Oxford University Press, 1987.

[11] Wolf, D., Keblinski, P., Phillpot, S. R., and Eggebrecht, J., "Exact Method for the Simulation of Coulombic System by Spherically Truncated, Pairwise r^{-1} Summation", J. Chem. Phys., Vol. 110, No. 17 (1999), pp. 8254-8282.

[12] Heslot, F., Cazabat, A. M., Levinson, P., and Fraysse, N., "Experiments on Wetting on the Scale of Nanometers: Influence of the Surface Energy", Phys. Rev. Lett., Vol. 65, No. 5 (1990), pp. 599-602.

[13] Young, J., Koplik, J., and Banavar, J. R., "Terraced Spreading of Simple Liquids on Solid Surfaces", Phys. Rev. A, Vol. 46, No. 12 (1992), pp. 7738-7749.

[14] Nieminen, J. A., Abraham, D. B., Karttunen, M., and Kaski, K., "Molecular Dynamics of a Microscopic Droplet on Solid Surface", Phys. Rev. Lett., Vol. 69, No. 1 (1992), pp. 124-127.

[15] Voué, M., and De Coninck, J., "Spreading and Wetting at the Microscopic Scale: Recent Developments and Perspectives", Acta Mater., Vol. 48 (2000), pp. 4405-4417.